Development of cascade enzymatic reaction-based nucleic acid detection method using personal glucose meter

Se Hee Jang

The Graduate School
Yonsei University
Department of Medical Device Engineering and Management

Development of cascade enzymatic reaction-based nucleic acid detection method using personal glucose meter

A Master's Thesis Submitted
to the Department of Medical Device
Engineering and Management
and the Graduate School of Yonsei University
in partial fulfillment of the
requirements for the degree of
Master of engineering

Se Hee Jang

December 2024

This certifies that the Master's Thesis
of Se Hee Jang is approved.

Thesis Supervisor Jae-Sung Kwon

Thesis Committee Member Eun-Jung Lee

Thesis Committee Member Jun Ki Ahn

The Graduate School
Yonsei University

December 2024

TABLE OF CONTENTS

LIST OF FIGURES

LIST OF FIGURES

ABSTRACT

Development of cascade enzymatic reaction-based nucleic acid detection method using personal glucose meter

This study presents a novel molecular diagnostic platform that integrates the structure-specific cleavage activity of flap endonuclease 1 (FEN1)-coupled cascade enzymatic reactions to detect target nucleic acids without the need for polymerase chain reaction (PCR) amplification. This system leverages AMP produced by FEN1 cleavage to trigger glucose degradation, which can be quantified using a personal glucose meter (PGM). Validation of this platform was conducted using target DNA based on the Chlamydia trachomatis (Ct) sequence, demonstrating effectiveness in detecting sequences identical to common bacterial pathogens. Utilizing this system, target nucleic acid was successfully detected with a detection limit of 4.8 pM. Additionally, the potential to detect target nucleic acids derived from Chlamydia trachomatis showed excellent selectivity compared to other STD genes and mismatches. By overcoming the limitations of PCR and fluorescence-based techniques, this platform offers a cost-effective, scalable, and user-friendly diagnostic solution with significant potential for application in resource-limited settings.

Key words : **Flap endonuclease 1, Cascade enzyme reaction, Personal glucose meter, Nucleic acid detection, point-of-care testing**

I. Introduction

1. Detection of Nucleic acid

Clinical medicine relies on examining symptoms, indicators, and diagnostic tests to detect illnesses and provide standard symptomatic treatments, which may not be effective for all patients.[1, 2] The global rise in aging populations and chronic diseases highlights the growing importance of early disease prevention.[3, 4, 5] Advances in information technology are transforming healthcare management, particularly in continuous patient monitoring and improving treatment accessibility.[6, 7]

Nucleic acid detection plays a crucial role in modern diagnostics by enabling the identification of pathogens, genetic disorders, and various diseases.[6, 7, 8, 9] These techniques have gained significant prominence in recent years due to their potential to advance personalized medicine, facilitate early disease detection, and allow for tailored treatments.[1, 4, 6] Among these methods, the polymerase chain reaction (PCR) has long been considered the gold standard for nucleic acid detection, due to its high sensitivity and ability to amplify small amounts of DNA.[10, 11, 12, 13]

2. Polymer Chain Reaction and Limitations of PCR

Over the years, PCR technology has significantly evolved, with advancements such as real-time PCR (qPCR) and digital PCR (dPCR), which offer improved sensitivity, quantification, and accuracy.[14, 15, 16] PCR-based methods allow the rapid and sensitive detection of specific genetic material by amplifying small amounts of DNA within a sample.[17, 18, 21] While these advancements have improved PCR performance, each generation of technology still presents certain limitations, which have spurred the development of new methods.

The first-generation PCR has limitations, such as the requirement for precise thermal cycling, and the complexity and cost of designing sophisticated probes. Additionally, the process of verifying results with gel after the reaction may have low resolution, hindering the detection of small restriction fragments.[19, 20] Second-generation quantitative real-time PCR (qRT-PCR), which measures fluorescence without using gels, requires dual-labeled probes with a fluorophore and a quencher, leading to higher costs. Moreover, qRT-PCR relies on standard curve quantification, where errors can result in inaccurate outcomes, potentially causing false positives.[22, 23, 24, 25] To address these drawbacks, third-generation digital PCR (dPCR) was developed. dPCR enhances quantification by partitioning DNA samples into individual reactions, providing higher precision without requiring standard curves.[22, 24, 26] Despite these advancements, dPCR and similar techniques

depend on expensive instrumentation and bulky equipment, limiting their use in point-of-care settings or resource-limited environments.

The need for specialized lab conditions and trained personnel further restricts their application in rapid or on-site diagnostics, highlighting the demand for more portable and cost-effective solutions. [27, 28, 29]

3. Personal Glucose Meter (PGM)

Point of Care Testing (POCT) refers to diagnostic testing performed immediately at the location where the patient is present.[30, 31] POCT can be conducted not only in hospitals or clinics but also in various settings such as ambulances, homes, and pharmacies.[32] A key feature of POCT is that samples do not need to be sent to a central laboratory; instead, healthcare professionals or patients themselves can perform the tests and obtain results immediately.[33, 34] This capability allows for quicker decision-making and treatment planning.

The personal glucose meter (PGM) is a portable, affordable device that provides reliable quantitative results and is easy to use, making it one of the representative devices for point-of-care testing.[35, 36] However, the primary limitation of the PGM is that it is restricted to detecting only glucose, which limits its application in detecting a broader range of biomarkers.[37, 38, 39, 40, 41] Pioneering research by Xiang and Lu in 2011 has led to the development of methods to adapt PGMs for detecting non-glucose targets.[40, 42,43, 44, 45, 46] These efforts aim to harness the PGM's portability and cost-effectiveness by linking the detection of various analytes to changes in glucose concentration, thereby expanding its diagnostic applications beyond glucose monitoring. However, these techniques often require complex procedures, such as immobilizing enzymes on oligonucleotides and using magnetic particles for separation and purification, making them challenging to implement in POCT settings.

4. Cascade Enzyme Reaction

A cascade enzyme reaction, also known as a multi-enzyme reaction or enzyme cascade, refers to a series of enzymatic reactions that occur sequentially in a single reaction vessel without isolating the intermediate products.[47] In this process, the product of one enzyme reaction serves as the substrate for the next enzyme in the sequence. This method increases reaction efficiency and intermediate handling, reducing costs and waste while providing higher yields and economic benefits.[48]

Flap endonuclease 1 (FEN1) plays a pivotal role as a structure-specific nuclease, serving as a central component in both DNA replication and repair mechanisms.[49, 50, 51] Upon replicating the upstream Okazaki fragment, the replication complex performs strand displacement synthesis, generating a 5' flap on the downstream fragment.[52] These flaps are cleaved at their bases by FEN1.

5. Objective of this study

Despite advancements in diagnostic techniques, existing methods still rely heavily on expensive and bulky equipment, limiting their use in point-of-care testing (POCT) and resource-limited environments. Additionally, the need for specialized laboratory settings and trained personnel restricts the feasibility of rapid, on-site diagnostics, highlighting the demand for more portable and cost-effective solutions. Although recent research has successfully adapted PGMs to detect non-glucose targets by linking analyte detection to changes in glucose concentration, these methods often require complex procedures like enzyme immobilization and magnetic particle separation, posing challenges for simple and scalable POCT implementation.

To overcome these limitations, this study aims to develop an innovative diagnostic platform by combining FEN1's structure-specific cleavage activity with a cascade enzymatic reaction (CER). By directly linking target DNA detection to glucose degradation, this platform enables easy analysis with a PGM, bypassing complex washing or labeling steps. This approach is designed to be both cost-effective and practical for a wide range of applications, particularly in settings where accessibility to conventional diagnostic resources is limited.

II. Materials and Methods

1. Materials

All synthetic sequences (Table 1, 2, 3) were purchased from Integrated DNA Technologies Inc. (Coralville, IA, USA), Adenosine 5′-monophosphate disodium salt, (Sigma-Aldrich, St. Louis, MO, USA), ADP Assay Kit (Colorimetric/Fluorometric) (abcam, Toronto, Canada), Myokinase from rabbit muscle (MK) (Sigma-Aldrich, St. Louis, MO, USA), Pyruvate Kinase from rabbit muscle (PK), Hexokinase from Saccharomyces cerevisiae (HK) (Sigma-Aldrich, St. Louis, MO, USA), Thermostable FEN1 (Enzynomics, Daejeon, Republic of Korea), 10X rCutsmart™, 10X ThermoPol® reaction buffer (New England Biolabs (NEB), Ipswich, MA, USA), Nuclease free water (NFW) (Integrated DNA Technologies, Coralville, IA, USA), Phospho(enol)pyruvic acid monopotassium salt (PEP) (Sigma-Aldrich, St. Louis, MO, USA), Glucose-6-phosphate Dehydrogenase from Leuconostoc mesenteroidess (Sigma-Aldrich, St. Louis, MO, USA), Human serum (Sigma-Aldrich, St. Louis, MO, USA).

Table 1. DNA sequences used in this work

Name	DNA sequence (5' → 3')[a]
Target DNA (Ct)	CAACAAGCTACCATTTCTTTCTCCCAGCTTAAGAACCGTCAGACAGAAAA
Q-probe	TTTCTGTCTGACGGTTCTTAA-(BHQ)
F-probe	**(FAN)-rA**GCTGGGAGAAAGAAATGGTAGCTTG
UP1	TTTCTGTCTGACGGTTCTT
UP2	TTTCTGTCTGACGGTTCTTA**C**
UP3	TTTCTGTCTGACGGTTCTTA**CA**
UP4	TTTCTGTCTGACGGTTCTTA**CAA**
UP5	TTTCTGTCTGACGGTTCTTA**CAAG**
UP6	TTTCTGTCTGACGGTTCTTA**CAAGTTAGAG**
UP7	TTTCTGTCTGACGGTTCTTA**CAAGTTAGAGGGAGG**
UP8	TTTCTGTCTGACGGTTCTTA**CAAGTTAGAGGGAGGGGGAT**
DP1	/5Phos/rAGCTGGGAGA
DP2	**/5Phos/rA**AAGCTGGGA
DP3	/5Phos/rAGCTG
DP4	/5Phos/rAGCTGG
DP5	/5Phos/rAGCTGGG
DP6	/5Phos/rAGCTGGGA
DP7	/5Phos/rAGCTGGGAG
DP8	/5Phos/rAGCTGGGAGAA
DP9	/5Phos/rAGCTGGGAGAAA
DP10	/5Phos/rAGCTGGGAGAAAG
DP11	/5Phos/rAGCTGGGAGAAAGA
DP12	/5Phos/rAGCTGGGAGAAAGAA
DP13	/5Phos/rAGCTGGGAGAAAGAAATGGT
DP14	/5Phos/rAGCTGGGAGAAAGAAATGGTAGCTTG
DP15	/5Phos/rAGCTGGGAGAAAGAAATGGTAGCTTGTTG

[a]The colors of the oligonucleotide sequences correspond to the domains depicted in Fig. 1. Purple letters represent the UP hybridized with the target DNA, while the bold orange letters in UP indicate the 3 ' -end flap. Green letters represent the DP hybridized with the target DNA, and red letters represent the AMP hybridized with the target DNA, the product of FEN1 cleavage. The bold red letters represent 5 '- end flap of DP.

Table 2. DNA sequences and DP/target DNA hybridization Tm used in Fig. 5 (c)

DP (5′-3′)[a]	Tm (°C)	Target DNA (5′-3′)[b]
/5Phos/rAATGATATAT	22	CAACAAGCTACCATTTCTT**ATATATCATT**TAAGAACCGTCAGACAGAAAA
/5Phos/rAACTATGATA	24	CAACAAGCTACCATTTCTT**TATCATAGTT**TAAGAACCGTCAGACAGAAAA
/5Phos/rAGATGATAGA	26	CAACAAGCTACCATTTCTT**TCTATCATCT**TAAGAACCGTCAGACAGAAAA
/5Phos/rAGTTGAGAGA	28	CAACAAGCTACCATTTCTT**TCTCTCAACT**TAAGAACCGTCAGACAGAAAA
/5Phos/rAGCTGAGAGA	32	CAACAAGCTACCATTTCTT**TCTCTCAGCT**TAAGAACCGTCAGACAGAAAA
/5Phos/rAGCTGGGAGA	33	CAACAAGCTACCATTTCTT**TCTCCCAGCT**TAAGAACCGTCAGACAGAAAA
/5Phos/rAGCCGGGAGA	34	CAACAAGCTACCATTTCTT**TCTCCCGGCT**TAAGAACCGTCAGACAGAAAA
/5Phos/rAGCCGGGAGC	36	CAACAAGCTACCATTTCTT**GCTCCCGGCT**TAAGAACCGTCAGACAGAAAA
/5Phos/rAGCCGGGCGC	38	CAACAAGCTACCATTTCTT**GCGCCCGGCT**TAAGAACCGTCAGACAGAAAA

[a]Green letters represent the DP hybridized with the target DNA, and red letters represent the AMP hybridized with the target DNA, the product of FEN1 cleavage. Bold sky-blue letters represent the part of the changed target DNA (Ct) sequence to hybridization with 10 mer DPs which have various Tm values. Navy letters represent the part of the don't change target DNA (Ct) sequence.

Table 3. DNA sequences used in selectivity experiment

Name	DNA sequence (5' → 3')[a]
MM1	CAACAAGCTACCATTTCTTTCTCCCAGCATAAGAACCGTCAGACAGAAAA
MM2	CAACAAGCTACCATTTCTTTCTCCCAGCAAAAGAACCGTCAGACAGAAAA
MM3	CAACAAGCTACCATTTCTTTCTCCCAGGAAAAGAACCGTCAGACAGAAAA
MM4	CAACAAGCTACCATTTCTTTCTCCCAGGATAAGAACCGTCAGACAGAAAA
MM5	CAACAAGCTACCATTTCTTTCTCCCACGATAAGAACCGTCAGACAGAAAA
Ureaplasma urealyticum (UU)	AGAGAAGCAAAAGTAATCAGCATTAAAAATACTGGTGACCGTCCTATCCA
Human papillomavirus(HPV)	GTTCTGCTCCATCTGCCACTACGTCTTCTAAACCTGCCAAGCGTGTGCGT
Candida albicans (CA)	GTTTGCTTGAAAGACGGTAGTGGTAAGGCGGGATCGCTTTGACAATGGC
Treponema pallidum (TP)	CATCATCAGGAAGGAAAAGACATCGCAGCGCTTACCCTCGCTCTGTTGAA
Neisseria gonorrhoeae (NG)	GATATCTGATTAGCTGGTTGGCGGGGTAAAGGCCCACCAAGGCGACGATC

[a]Blue letters represent the part of mismatches.

2. FEN1 cleavage activity and verify ADP creation

To prepare the FEN1 cleavage reaction solution, 0.1 μM Q-primer, 50 nM F-primer, 60 nM target DNA, 0.4 U/μL FEN1, and 1X ThermoPol® reaction buffer was combined. The mixture was then incubated at 45 °C for 60 minutes. Fluorescence emission spectra were recorded from 510 nm to 620 nm at an excitation wavelength (λ_{ex}) of 525 nm, using an Infinite 200 Pro Multi-Mode Microplate Reader (Tecan, Männedorf, Switzerland) in fluorescence intensity scan mode.

For the ADP assay, the ADP standard solution was prepared according to the ADP Assay Kit protocol. The reaction mixture consisted of 10 μM UP, 10 μM DP2, 5 μM target DNA, 1.28 U/μL FEN1, 0.8 U/μL MK, 2 mM PEP, 4 mM glucose, and 1X rCutsmart™ reaction buffer, and was incubated at 45 °C for 120 minutes. Afterward, 50 μL of this reaction solution was combined with 50 μL of the ADP standard solution and mixed with the fluorescence reaction solution. This mixture was then incubated in the dark at room temperature for 30 minutes, and the fluorescence emission was measured from 570 nm to 670 nm at an excitation wavelength (λ_{ex}) of 587 nm, using the same Tecan Infinite 200 Pro Multi-Mode Microplate Reader in fluorescence intensity scan mode.

3. Buffer Selection for one-step System

The FEN1 cleavage reaction solution composition and measurement conditions are the same as those listed above, but the concentration ratios of the rCutsmart™ and ThermoPol® reaction buffer solutions are varied. MK and CER reaction solution was prepared by mixing, 0.8 U/μL MK, 0.1 U/μL HK, 0.1 U/μL PK, 2 mM PEP, 4 mM glucose, and various concentration ratios of the rCutsmart™ and ThermoPol® reaction buffer solutions. After incubation at 45 °C for 60 min and enzyme inactivated at 95 °C for 10 minutes. Then 6 μL of the reaction solution glucose concentration was measured with the PGM (Accu-Chek Active, Roche, Basel, Switzerland).

4. Confirmation of CER results according to UP/DP

1X rCutsmart™ reaction buffer, 5 μM UP, 5 μM DP, 2 mM PEP, 4 mM glucose, 0.1 U/μL HK, 0.1 U/μL PK, 1.28 U/μL FEN 1, 0.4 U/μL MK, and 2.5 μL of target DNA at varying concentrations were prepared for optimization of UP and DP hybridization form and length. A mixture of 1X rCutsmart™ reaction buffer, 2 mM PEP, 4 mM glucose, and varying concentrations of UP, DP, HK, PK, FEN1, MK, and target DNA was prepared. The above reaction mixtures were incubated at 45 °C for 120 min. The resulting glucose level was measured using PGM.

5. Sensitivity and selectivity

1X rCutsmart™, 2 mM PEP, 4 mM glucose, 1.28 U/μL of FEN1, 0.4 U/μL of MK, 2.5 U/μL of PK/HK, 2.5 μM of UP/DP and various concentrations of target DNA were prepared sensitivity reaction solution. Selectivity was confirmed using 1 nM mismatched target DNA and non-target DNA. The above reaction mixtures were incubated at 45 ℃ for 120 min and the enzyme was inactivated at 95 ℃ for 10 min. The resulting glucose level was measured using PGM.

6. Detection of Target DNA in 1% Human Serum

1X rCutsmart™, 2 mM PEP, 4 mM glucose, 1.28 U/μL of FEN1, 0.4 U/μL of MK, 2.5 U/μL of PK/HK, 2.5 μM of UP/DP and various concentrations of target DNA were prepared sensitivity reaction solution. The target DNA was diluted at 1% human serum. The above reaction mixtures were incubated at 45 ℃ for 120 min and the enzyme was inactivated at 95 ℃ for 10 min. They analyzed using the same method mentioned earlier to detect the target DNA.

III. Results and Discussion

1. Basic Principles

The basic principle of a platform to detect the target DNA based on the FEN1-assisted cascade enzymatic reaction is depicted in Figure 1. Two probes, an upstream probe (UP) and downstream probe (DP), are specifically designed to hybridize with the target DNA sequence. The DP contains adenine ribonucleotide (rA) at its 5′-terminus. On binding to target DNA, the UP invades the duplex formed between the DP and the target DNA, creating a flap structure. This structure allows FEN1 to recognize and cleave the 3′ flap of the UP just after the first base pair preceding the 5′ flap of the DP, resulting in the formation of AMP (adenosine monophosphate) as a cleavage product. This enzymatic cleavage initiates a cyclic reaction, as the melting temperature of the DP/target DNA duplex is lower than the reaction temperature, causing the cleaved DP to dissociate and be replaced by an intact DP, facilitating continuous cleavage cycles by FEN1. Following cleavage, the resultant AMP is phosphorylated by myokinase (MK) to generate ADP (adenosine diphosphate), which then serves as a substrate for cascade enzymatic reaction catalyzed by pyruvate kinase (PK) and hexokinase (HK), converting glucose to glucose-6-phosphate (G6P). The reduction in glucose concentration is subsequently measured using a portable glucose meter (PGM).

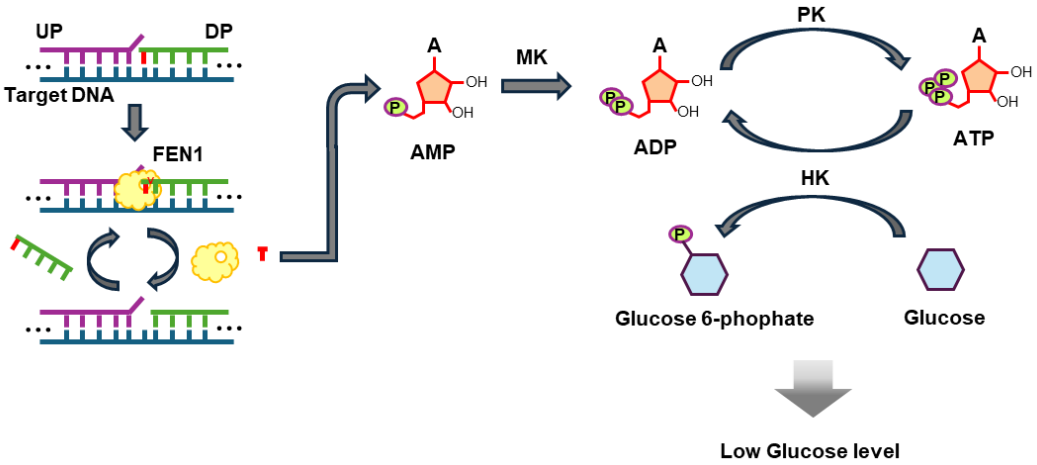

Figure 1. Schematic illustration of the FEN1-facilitated cascade enzymatic reaction system for detecting nucleic acids with a personal glucose meter (PGM).

2. FEN1 Cleavage Activity and Verification ADP Production

To verify the cleavage activity of FEN1, a FAM-labeled downstream probe (F-probe) and a BHQ-labeled upstream probe (Q-probe) were used to measure fluorescent signals. As shown in Figure 2(a), a high fluorescence signal was observed in the presence of only the F-probe and the template. However, upon the addition of the Q-probe, the fluorescence signal decreased significantly, indicating that the BHQ modified at the 3′ end of the Q-probe quenches the fluorescence signal of the FAM modified at the 5′ end of the F-probe. Interestingly, when FEN1 was added, the fluorescence signal increased to the same level as observed with only the F-probe and the template, indicating that the 5’ flap modified with FAM was cleaved by FEN1.

Next, a conventional ADP assay kit was employed to verify whether the cleaved flap from the rA-modified upstream probe by FEN1 is AMP. It was assumed that the portion cleaved from the flap of the downstream probe, which is modified with rA at the 5′ end, would be AMP due to FEN1 activity. If AMP were successfully converted to ADP by Myokinase (MK), it was expected to be detectable using the ADP assay kit. Using 5 μM of target DNA and 10 μM of upstream and downstream probes, the result showed a fluorescence signal corresponding to 4.4 μM on the standard curve of the ADP assay kit (Figure 2(b)), confirming that FEN1 cleaved one nucleotide (rA) from the 5′ end of the downstream probe and that AMP was successfully converted to ADP.

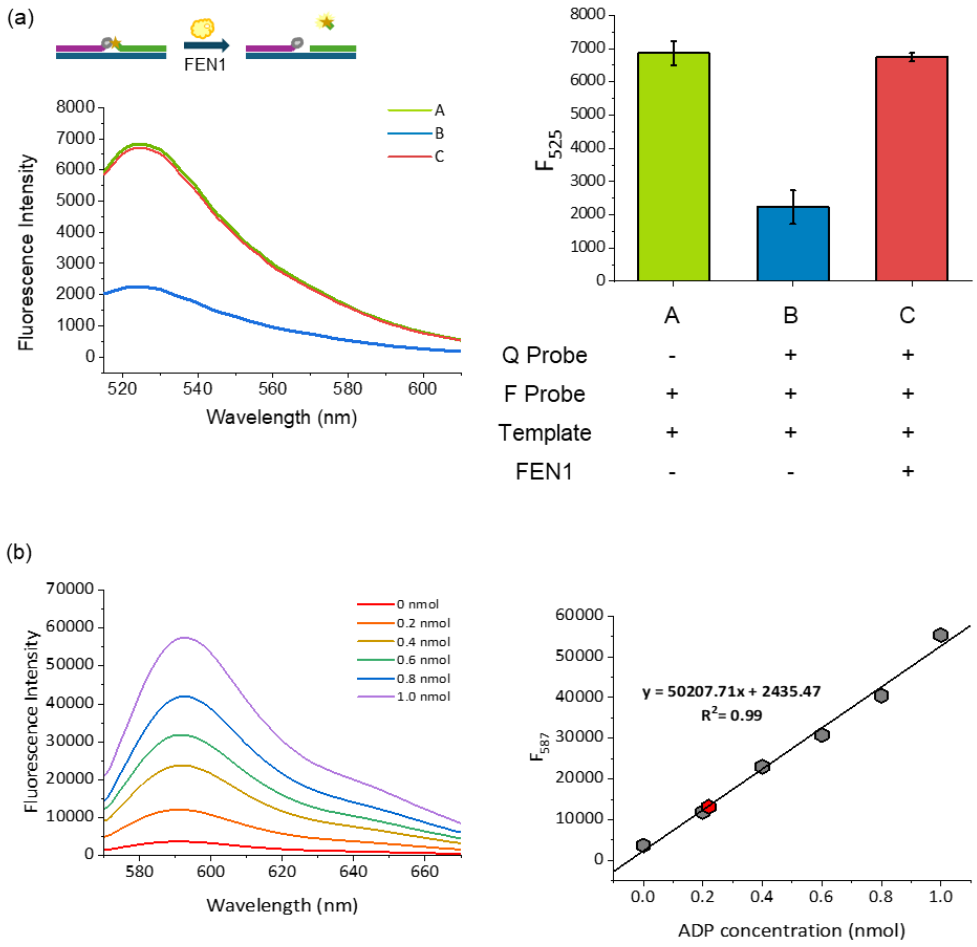

Figure 2. FEN1 cleavage activity and verify ADP creation. (a) Fluorescence emission spectra and fluorescence intensities at 525 nm (F525) with or without FEN1, Q-probe, and templates. (A) without quenching, (B) with quenching by Q-probe, and (C) restoration of fluorescence after FEN1 cleavage. (b) ADP assay kit results through FEN1 and MK reaction. Standard curve for ADP detection based on fluorescence intensity at 587 nm wavelength, with a calculated ADP concentration of 4.4 μM from the assay.

3. Buffer Selection for one-step System

This study aimed to select the optimal buffer for the developed system. FEN1 was used with ThermoPol® buffer, while the buffer for the cascade enzymatic reaction (CER) utilizing AMP as a substrate, along with Myokinase (MK), Pyruvate Kinase (PK), and Hexokinase (HK), had been previously established as rCutsmart™ buffer in earlier studies.[44, 67] The ratio of ThermoPol® and rCutsmart™ buffers was adjusted to evaluate their effects on the FEN1 cleavage reaction and the CER using AMP as a substrate. As shown in Figure 3(a), the glucose change level dropped significantly with even a small addition of ThermoPol® buffer, indicating that this buffer critically inhibits the CER. On the other hand, the FEN1 cleavage reaction exhibited the highest activity in ThermoPol® buffer, while significant activity was also observed in rCutsmart™ buffer (Figure 3(b)). Therefore, to achieve a one-step system, rCutsmart™ buffer was ultimately selected.

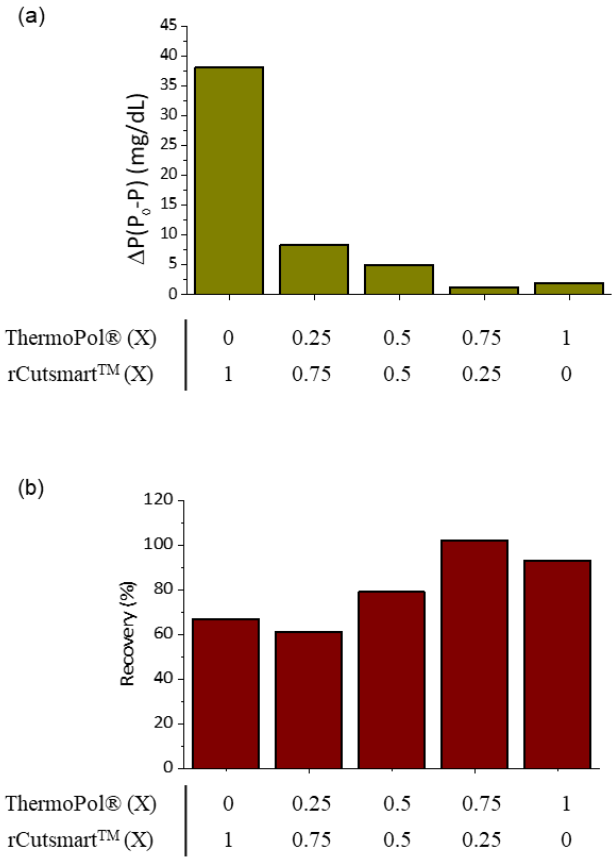

Figure 3. Assessment of buffer formulations with different proportions of ThermoPol® and rCutsmart™ for FEN1 activity and cascade enzymatic reaction (CER) efficacy. (a) Changes in PGM signal (ΔP) observed from the CER utilizing AMP as the substrate. (b) Percentage recovery determined by comparing the fluorescence signal restored post-FEN1 cleavage to the fluorescence signal from the F-probe alone. PGM signal change (ΔP) is defined as $P_0 - P$ (P_0 and P represent the PGM signal without target DNA and with target DNA). Recovery was calculated (C value/A value) x100.

4. Investigation of FEN1 cleavage activity on flap structure of UP and DP

In this system, the final glucose level measured by the PGM is determined by AMP production through one nucleotide cleavage catalyzed by FEN1. Therefore, AMP generation activity was verified based on the flap structures of UP and DP. Changes in glucose levels were measured through the FEN1-assisted CER reaction under four different conditions: a) no flap structure (UP1 and DP1), b) a flap at the 3′ end of UP (UP2 and DP1), c) a flap at the 5′ end of DP (UP1 and DP2), and d) flaps at both the 3′ end of UP and the 5′ end of DP (UP2 and DP2). As shown in Figure 4, a significant change in the PGM signal was observed regardless of the flap structure when the target DNA concentration exceeded 10 nM. However, at a low concentration (1 nM) of target DNA, the high PGM signal change was maintained only in the presence of a flap at the 3′ end of UP, while no further PGM signal change was observed with other flap structures. Therefore, a flap at the 3′ end of UP (UP2 and DP1) was ultimately selected as the probe for this system. Interestingly, the experimental results are consistent with previous findings reported by Kao et al.[54] They also claimed that the optimal condition for one nucleotide cleavage by FEN1 occurs when the UP has a 1 bp flap at the 3′ end and the DP lacks a flap at the 5′ end.

Next, to optimize the UP flap and DP lengths for this system, a range of UPs with varying 3′ end flap lengths (0–20 bp) and DP lengths (5–29 bp) was measured. The PGM signal change was then assessed, confirming that a 10 bp DP is optimal (Figure 5(a), (b)). This result, indicating that a 10 bp DP is optimal, could be explained by the concept of UP/target DNA complex recycling. The DP used had a Tm (melting temperature) of approximately 33 °C. Since the system operates at 45 °C, the Tm being lower than the reaction temperature likely allows the cleaved DP to dissociate from the UP/target DNA complex and be replaced by a fresh DP, enabling continuous FEN1 cleavage. To validate this hypothesis, the DP length was fixed at 10 bp, and DPs and template DNAs with varying Tm values were designed (Figure 5(c)). The results confirmed a sharp decrease in reactivity when the DP had a Tm below 26 °C or above 34 °C. At Tm values below 26 °C, the DP could not hybridize efficiently to the target DNA at the reaction temperature (45 °C), inhibiting the FEN1 cleavage reaction. Conversely, at Tm values above 34 °C, the cleaved DP failed to dissociate from the target DNA, reducing cleavage efficiency due to insufficient UP/target DNA complex recycling.

Furthermore, to maximize the performance, several reaction conditions were optimized by measuring the PGM signal change (Figure 6). Finally, the optimal conditions were determined to be a reaction temperature of 45 °C, 1.28 U/μL of FEN1, 0.4 U/μL of MK, 2.5 U/μL of PK/HK, 2.5 μM of UP/DP, and a reaction time of 90 min.

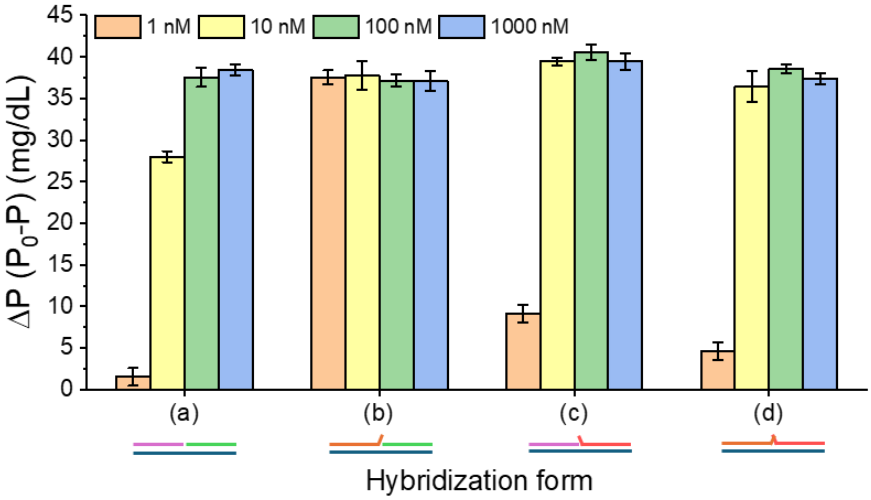

Figure 4. Changes in the PGM signal were evaluated based on the type of hybridization between UP/DP and the target DNA. The conditions examined included: (A) no flap structure (UP1 and DP1), (B) a flap at the 3′ end of UP (UP2 and DP1), (C) a flap at the 5′ end of DP (UP1 and DP2), and (D) flaps present at both the 3′ end of UP and the 5′ end of DP (UP2 and DP2). (For detailed sequences of the target DNA, UP, and DP, refer to Table 1.)

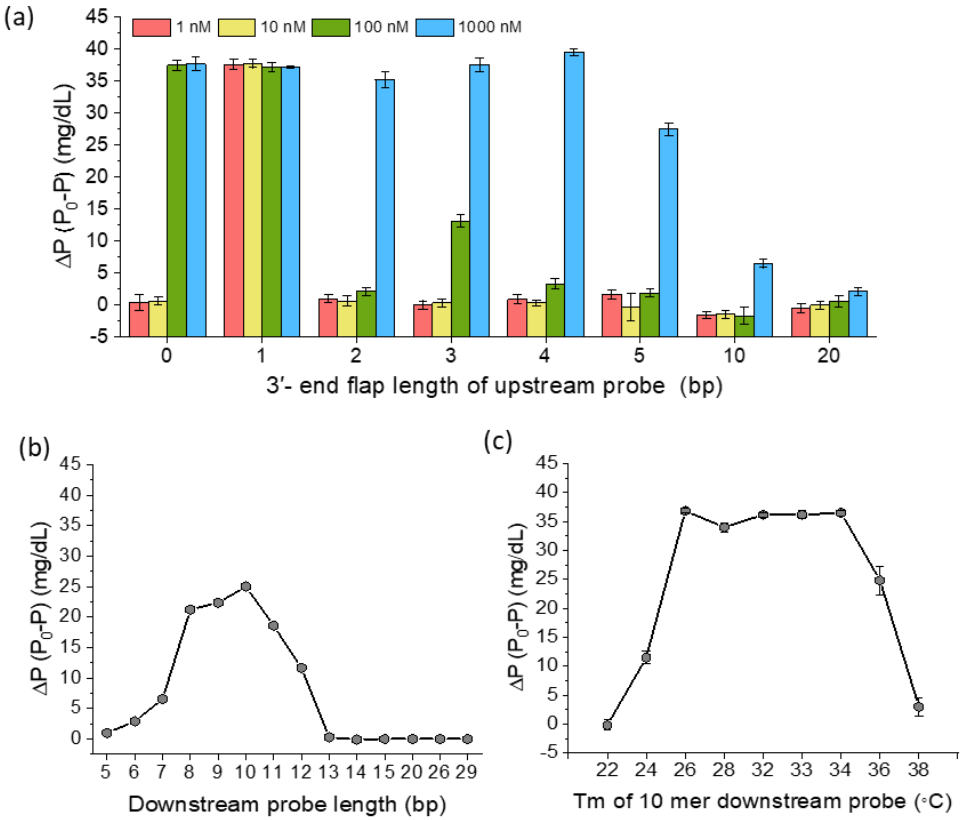

Figure 5. (a) Changes in the PGM signal (ΔP) as a function of the 3′ end flap length of UP (UP1−UP8) were analyzed at different target DNA concentrations (1 nM, 10 nM, 100 nM, and 1 μM). Additionally, PGM signal changes (ΔP) were assessed as a function of (b) the length of DP (DP1−DP15) and (c) the melting temperature (Tm) of various 10 bp DPs. (For detailed sequences of UP and DP probes, see Table 1 and 2.)

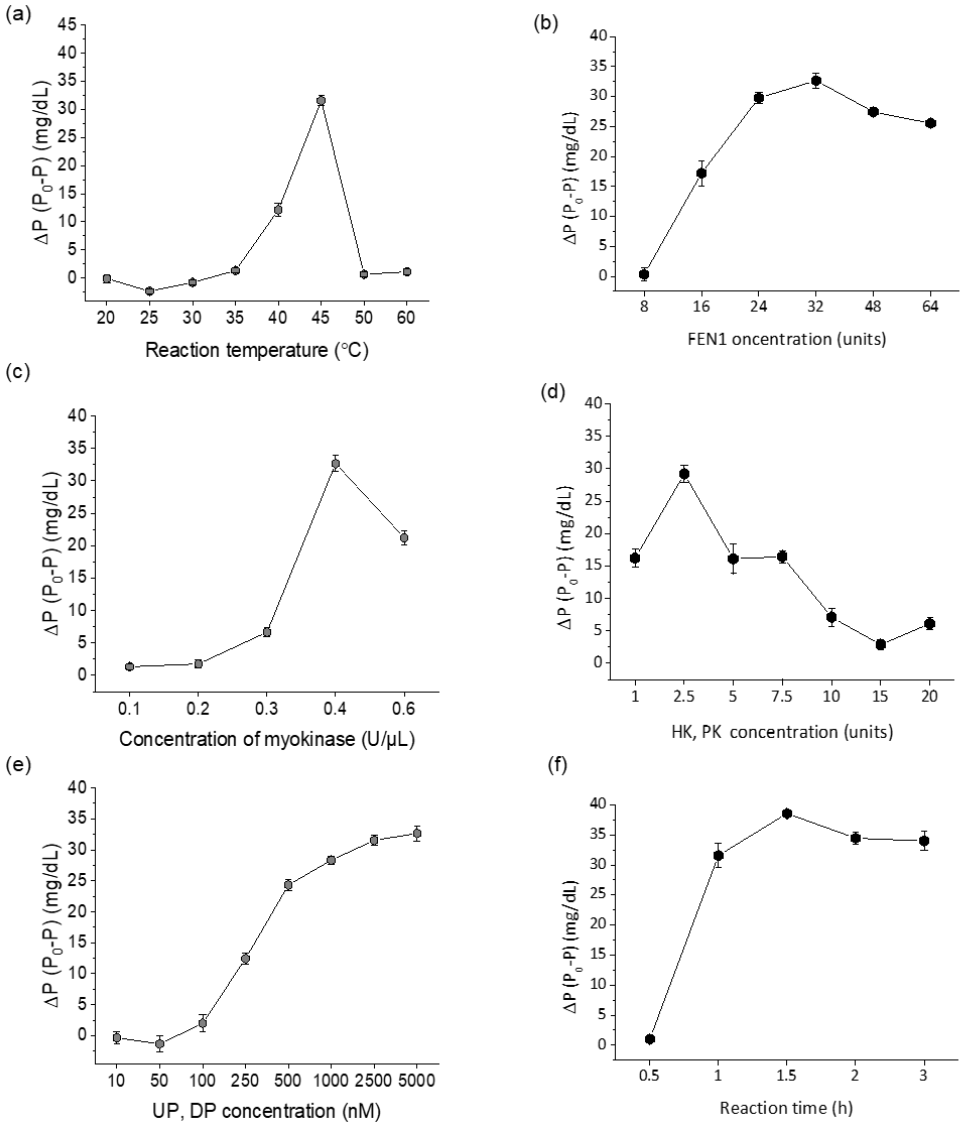

Figure 6. Optimization of (a) temperature (5 μM UP, 5 μM DP, 0.1 U/μL HK, 0.1 U/μL PK, 1.28 U/μL FEN 1, 0.4 U/μL MK, and react for 1 h), (b) concentration of FEN1 (5 μM UP, 5 μM DP, 0.1 U/μL HK, 0.1 U/μL PK, 0.4 U/μL MK, and react at 45 ℃ for 1 h), (c) concentration of MK (5 μM UP, 5 μM DP, 0.1 U/μL HK, 0.1 U/μL PK, 1.28 U/μL FEN 1, and react at 45 ℃ for 1 h) (d) concentration of HK, PK (5 μM UP, 5 μM DP, 0.4 U/μL MK, 1.28 U/μL FEN 1, and react at 45 ℃ for 1 h), (e) concentration of UP, DP (0.1 U/μL HK, 0.1 U/μL PK, 0.4 U/μL MK, 1.28 U/μL FEN 1, and react at 45 ℃ for 1 h), (f) reaction time (2.5 μM UP, 2.5 μM DP, 0.1 U/μL HK, 0.1 U/μL PK, 1.28 U/μL FEN 1, 0.4 U/μL MK, and react at 45 ℃)

5. Performance of system

Under optimized reaction conditions, sensitivity was assessed (Figure 7). Serially diluted target DNA samples were prepared and tested for activity by measuring changes in the PGM signal according to the target DNA concentration. The change in PGM signal increased with rising target DNA concentrations, demonstrating a linear correlation with concentrations from 0 to 100 pM ($\Delta P = 0.308$ x [target DNA] (pM) + 0.166, $R^2 = 0.98$; $\Delta P = P0 - P$, where P_0 and P represent the PGM signals in the absence and presence of target DNA, respectively). Based on the $3\sigma/S$ rule for the inset in Figure 7, where σ is the standard deviation of the blank and S is the slope, the limit of detection (LOD) was determined to be 4.8 pM. This sensitivity is either lower than or comparable to previously reported PGM-based nucleic acid detection methods (Table 4). Additionally, the method offers simplicity as a one-step, washing-free, isothermal approach, requiring only the mixing of the sample with the reaction mixture.

Furthermore, the selectivity of the system was assessed by examining the extent of PGM signal changes in response to various sexually transmitted disease (STD)-related DNA (UU, HPV, CA, TP, and NG) as non-target DNA under the same conditions. As shown in Figure 8, a significant change in PGM signal was observed only with the target DNA (Ct), while other non-target DNAs produced only minor PGM signal changes similar to the blank. Additionally, the system was tested with 1–3 bp mismatches (MM1–MM5) in the target DNA (Table 3). Interestingly, at a concentration of 1 nM, no PGM signal change was detected for MM2–MM5 during the reaction, while the presence of a single base mismatch near the flap structure (MM1) exhibited almost no difference in PGM signal change compared to the target DNA (Figure 9(a)). The effect of concentration on the PGM signal change was further investigated for both the target DNA and MM1, demonstrating a clear distinction in PGM signal change at concentrations below 100 pM (Figure 9(b)). These findings indicate that the system exhibits high selectivity for the target nucleic acid and has the potential to distinguish mutations within the linear detection range.

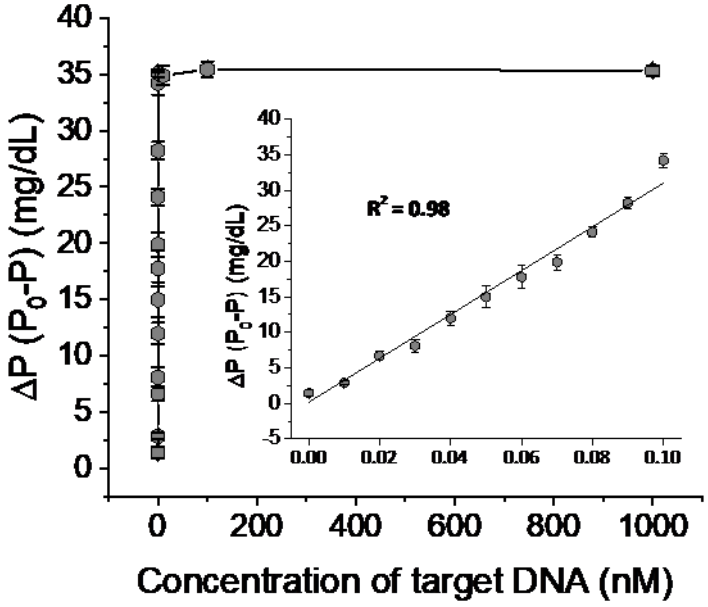

Figure 7. The sensitivity of the system for detecting target DNA concentrations is presented. (Inset) A linear relationship is observed between PGM signal change (ΔP) and target DNA concentration (0−100 pM).

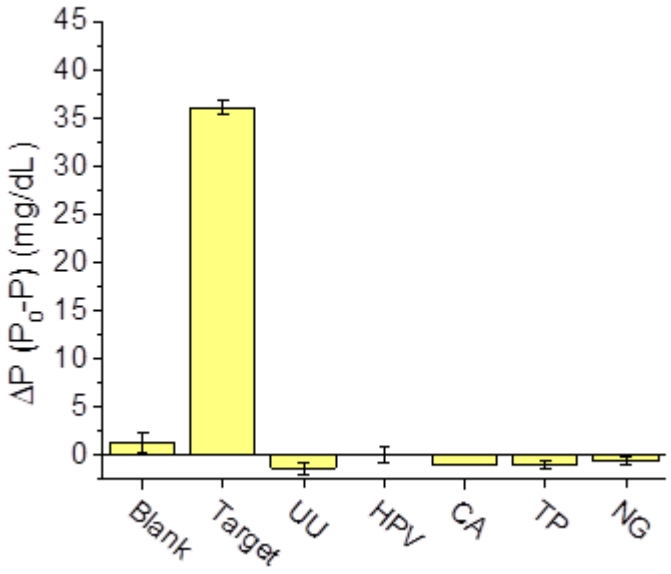

Figure 8. Specificity of the system for target DNA detection is demonstrated through PGM signal changes (ΔP) for the target DNA (Ct) in comparison to non-target DNAs, including UU (Ureaplasma urealyticum), HPV (Human papillomavirus), CA (Candida albicans), TP (Treponema pallidum), and NG (Neisseria gonorrhoeae). (Detailed sequences are provided in Table 3.)

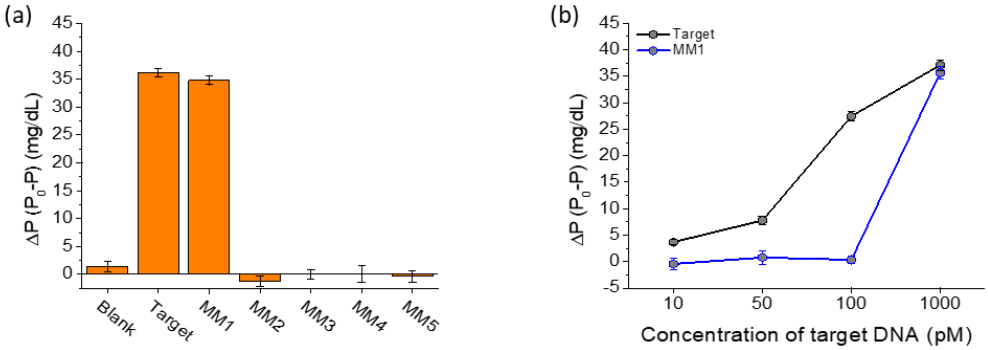

Figure 9. Selectivity of the system for detecting target DNA and single-base mismatches is illustrated. (a) PGM signal changes (ΔP) for the target DNA and mismatch sequences (MM1–MM5) are presented. (Detailed sequences of the mismatch sequences can be found in Table 3.) (b) PGM signal changes for the target DNA and MM1 at varying concentrations reveal a clear distinction at lower concentrations (10 pM–1 nM).

Table 4. Comparison of Limit of Detection (LOD) and reaction times for detection of target DNA from various previous research.

Ref.	LOD	Assay time	The number of step	Reaction temperature
[57]	40 pM	30 min	2	Room temperature (RT)
[58]	10^2 copies	65 min	2	58~95 ℃/ 30 ℃
[59]	10 copies	34 min	2	58~95 ℃/ RT
[60]	100 pM	63 min	3	RT
[61]	0.36 pM	100 min	2	RT/ 55 ℃
[62]	98 pM	150 min	2	37 ℃, 50 ℃
[46]	10 pM	60 min	2	RT
[63]	2.6 fM	155 min	3	16~95°C
[64]	2.4 and 1.1 pM	150 min	3	RT/ 37 ℃, 50 ℃
[65]	0.26 pM	10 h	3	RT
[66]	57 pM	240 min	3	37 ℃
[44]	27 pM	120 min	2	35 ℃, 37 ℃
This work	4.8 pM	120 min	1	45 ℃

The table summarizes the performance metrics, including LOD and reaction time, reported in studies that detect the same or similar target DNA as the current study. The references are provided for each comparison.

6. Practical applicability

To assess the practicality of the system in clinical applications, spiked human serum samples with varying concentrations of target DNA were analyzed. As shown in Figure 10, a linear correlation ($R^2 = 0.99$) was observed between PGM signal changes and target DNA concentration in a complex 1% human serum matrix. Utilizing this calibration curve, target DNA concentrations were precisely measured, achieving a coefficient of variation (CV) of less than 3% and recovery rates ranging from 99.9% to 102.4% (Table 5). In summary, these results affirm the potential of this assay for reliable miRNA sensing in real biological fluids, demonstrating its suitability for analyzing biological samples.

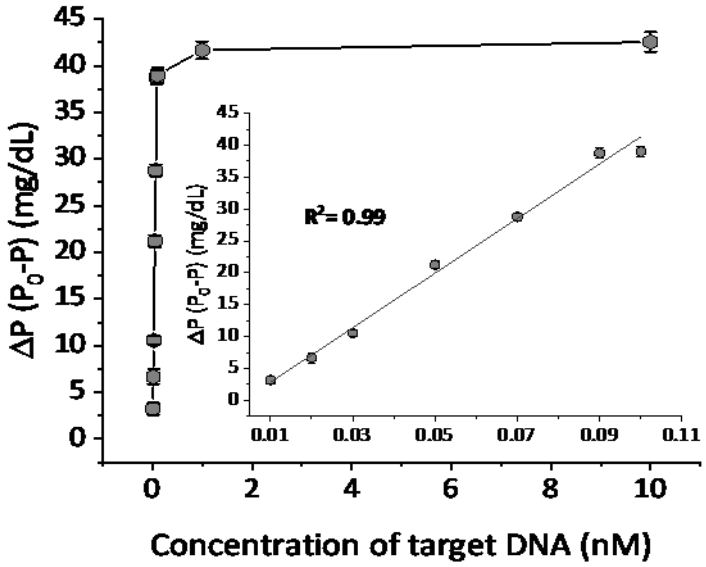

Figure 10. The relationship between the changes of the PGM signal and the concentration of target DNA spiked in diluted human serum (1%). (Inset) Linear range between PGM signal change and target DNA concentration (0−100 pM)

Table 5. Determination of target DNA in diluted human serum (1%)

Added target DNA (pM)	Measured target DNA (pM)[a]	SD[b]	CV[c] (%)	Recovery[d] (%)
40	39.97	1.05	2.62	99.9
60	61.46	0.81	1.31	102.4
80	80.03	0.93	1.16	100.03

[a] Mean of three measurements.

[b] Standard deviation of three measurements.

[c] Coefficient of variation = SD/mean × 100.

[d] Measured value/added value × 100

IV. Discussion

The results presented in this study highlight the effective application of FEN1 in a cascade enzymatic reaction (CER) system for the detection of target DNA. Findings confirm the cleavage activity of FEN1 through fluorescence assays, where the restoration of fluorescence signals indicates successful cleavage of the 5′ flap. Moreover, the subsequent conversion of the cleaved AMP to ADP by Myokinase (MK) further demonstrates the functionality of the enzyme in generating detectable products, affirming the suitability of this enzymatic system for DNA analysis.

In the optimization of reaction conditions, it was identified that the balance of enzyme buffers is crucial for maximizing the activity of FEN1 and MK. The choice of rCutsmart buffer was validated as it enabled FEN1 to retain activity while supporting the functionality of MK and other enzymes involved in the CER. Thus, experiments underscore the importance of optimizing buffer conditions, as the efficiency of enzyme interactions directly influences the overall reaction yield.

The investigation into the binding configurations of the upstream (UP) and downstream (DP) probes corroborates previous studies by Kao et al.[54], emphasizing the necessity of a 1 nt flap on the UP for optimal FEN1 activity. The observed signal differences linked to the presence and length of flaps further confirm that FEN1's recognition mechanism is sensitive to structural nuances in the DNA substrates. In addition, the optimal length of the DP was found to be 10 mers, highlighting the critical role of Tm values in ensuring proper binding and recycling of oligonucleotides during the reaction.

Through comprehensive optimization of enzyme concentrations, reaction temperatures, and times, a robust system capable of generating significant signal changes for target DNA detection was achieved. Notably, findings suggest that a reaction temperature of 45°C provides a sweet spot that balances the activities of FEN1 and MK, despite their differing optimal temperatures. Furthermore, the optimization of MK concentration is particularly crucial due to its role in catalyzing the reversible reaction between ADP and AMP. At higher concentrations of MK, the reverse reaction from AMP to ADP is favored, which can decrease the overall conversion rate from AMP, emphasizing the importance of carefully balancing enzyme concentrations within the reaction. This balance is vital not only for MK but also for other enzymes involved in the cascade reaction, as their interactions and efficiency significantly impact the overall performance of the system. The calculated limit of detection (LOD) of 4.8 pM underscores the sensitivity of this system, which is particularly promising for applications requiring precise nucleic acid quantification.

Selectivity tests demonstrated the system's ability to distinguish between target DNA and mismatched or non-target sequences, affirming the potential for specific applications in mutation detection and diagnostic purposes. The minimal signal variations observed with mismatched bases and other non-target DNAs indicate a high degree of specificity, making this approach a valuable tool for genetic analysis.

Finally, the successful detection of target DNA in human serum validates the practical applicability of this system in clinical settings. The observed linear relationship and high recovery rates indicate that this method can reliably be employed in complex biological matrices, facilitating its potential use in diagnostic and therapeutic monitoring.

Overall, this study illustrates a streamlined and effective approach for nucleic acid detection that leverages the enzymatic cascade reaction mechanism, offering a significant advancement in the field of molecular diagnostics. Future work could explore the integration of this system with other molecular assays, further enhancing its versatility and application scope.

V. Conclusion

In the past, medical practices focused primarily on diagnosing diseases and treating them. However, there has been a paradigm shift towards predicting and preventing diseases based on patients' genetic information. This shift has been further emphasized by the growing importance of disease prevention and personalized treatment due to the aging population and the rise in chronic diseases. In this context, nucleic acid detection technologies play a pivotal role.

PCR, one of the most widely used nucleic acid detection technologies, is a molecular biology technique that amplifies specific DNA sequences. It has evolved from first-generation conventional PCR to second-generation real-time PCR and third-generation digital PCR, significantly improving accuracy, sensitivity, and automation. Nevertheless, limitations in terms of usage environment and accessibility remain a challenge.

Meanwhile, one of the most commonly used in vitro diagnostic devices, the blood glucose meter, offers the advantage of being easily accessible and user-friendly. However, its analytical capabilities are limited to measuring glucose levels. This study aimed to leverage the strengths of blood glucose meters and designed an enzyme cascade reaction-based nucleic acid detection system.

Specifically, a method was proposed that utilizes AMP, a cleavage product of FEN1, as a trigger to detect target DNA through an enzyme cascade reaction (CER) involving MK, PK, and HK. By employing probes (UP and DP) that specifically bind to the target DNA, a reduction in glucose levels was observed when the target DNA was present, which could be monitored using a personal glucose meter (PGM). This approach demonstrated selective detection of target DNA down to a concentration of 4.8 pM. Furthermore, it was confirmed that this detection method functions reliably in human serum.

This study suggests the potential for developing in vitro diagnostic devices. Future optimization of enzymes and reaction buffers to enhance sensitivity is expected to improve the feasibility of commercialization further. Additionally, systematic research on variations in glucose concentration and PGM signal differences across individuals and disease states could improve the precision of this system. With such advancements, this platform could become a widely utilized in vitro diagnostic tool in everyday life. These subsequent studies are anticipated to contribute to faster and more accurate diagnostics in clinical settings.

References

1. Ahmed, Z., Zeeshan, S., Mendhe, D., & Dong, X. (2020). Human gene and disease associations for clinical-genomics and precision medicine research. Clinical and translational medicine, 10(1), 297-318.

2. Guzman, N. A., & Guzman, D. E. (2021). Immunoaffinity capillary electrophoresis in the era of proteoforms, liquid biopsy and preventive medicine: a potential impact in the diagnosis and monitoring of disease progression. Biomolecules, 11(10), 1443.

3. Barbazzeni, B., & Friebe, M. (2022). Prevention, Prediction, Personalization, and Participation as Key Components in Future Health. In Novel Innovation Design for the Future of Health: Entrepreneurial Concepts for Patient Empowerment and Health Democratization (pp. 147-152). Cham: Springer International Publishing.

4. Razzak, M. I., Imran, M., & Xu, G. (2020). Big data analytics for preventive medicine. Neural Computing and Applications, 32(9), 4417-4451.

5. Razzak, I., Eklund, P., & Xu, G. (2022). Improving healthcare outcomes using multimedia big data analytics. Neural Computing and Applications, 34(17), 15095-15097.

6. Gammall, J., & Lai, A. G. (2022). Pan-cancer prognostic genetic mutations and clinicopathological factors associated with survival outcomes: a systematic review. NPJ Precision Oncology, 6(1), 27.

7. Lattanzi, W., Ripoli, C., Greco, V., Barba, M., Iavarone, F., Minucci, A., ... & Parolini, O. (2021). Basic and preclinical research for personalized medicine. Journal of Personalized Medicine, 11(5), 354.

8. Raza, A., Rustam, F., Siddiqui, H. U. R., Diez, I. D. L. T., Garcia-Zapirain, B., Lee, E., & Ashraf, I. (2022). Predicting genetic disorder and types of disorder using chain classifier approach. Genes, 14(1), 71.

9. Lee, C. Y., Jang, H., Kim, H., Jung, Y., Park, K. S., & Park, H. G. (2019). Sensitive detection of DNA from Chlamydia trachomatis by using flap endonuclease-assisted amplification and graphene oxide-based fluorescence signaling. Microchimica Acta, 186, 1-7.ISO 690

10. Saiki, Randall K., et al. "Enzymatic amplification of β-globin genomic sequences and restriction site analysis for diagnosis of sickle cell anemia." Science 230.4732 (1985): 1350-1354.

11. Saiki, R. K., Gelfand, D. H., Stoffel, S., Scharf, S. J., Higuchi, R., Horn, G. T., ... & Erlich, H. A. (1988). Primer-directed enzymatic amplification of DNA with a thermostable DNA polymerase. Science, 239(4839), 487-491.

12. Amos, J., & Patnaik, M. (2002). Commercial molecular diagnostics in the US: The Human Genome Project to the clinical laboratory. Human mutation, 19(4), 324-333.

13. Oliveira, M. C., Scharan, K. O., Thomés, B. I., Bernardelli, R. S., Reese, F. B., Kozesinski-Nakatani, A. C., ... & Réa-Neto, Á. (2023). Diagnostic accuracy of a set of clinical and radiological criteria for screening of COVID-19 using RT-PCR as the reference standard. BMC Pulmonary Medicine, 23(1), 81.

14. Mirza, A. H., Das, S., Pingle, M. R., Rundell, M. S., Armah, G., Gyan, B., ... & Golightly, L. M. (2018). A Multiplex PCR/LDR assay for viral agents of diarrhea with the capacity to genotype rotavirus. Scientific Reports, 8(1), 13215.

15. Varona, M., & Anderson, J. L. (2021). Advances in mutation detection using loop-mediated isothermal amplification. ACS omega, 6(5), 3463-3469.

16. Ahrberg, C. D., Ilic, B. R., Manz, A., & Neužil, P. (2016). Handheld real-time PCR device. Lab on a Chip, 16(3), 586-592.

17. Gautam, A. K., & Kumar, S. (2020). Techniques for the detection, identification, and diagnosis of agricultural pathogens and diseases. In Natural remedies for pest, disease and weed control (pp. 135-142). Academic Press.

18. Kaltenboeck, B., & Wang, C. (2006). Advances in real-time PCR: Application to clinical laboratory diagnostics. Advances in clinical chemistry, 40, 219.

19. Wang, Q., Zhang, X., Zhang, H. Y., Zhang, J., Chen, G. Q., Zhao, D. H., ... & Liao, W. J. (2010). Identification of 12 animal species meat by T-RFLP on the 12S rRNA gene. Meat Science, 85(2), 265-269.

20. Galal-Khallaf, A., Mohammed-Geba, K., Osman, A. G., AbouelFadl, K. Y., Borrell, Y. J., & Garcia-Vazquez, E. (2017). SNP-based PCR-RFLP, T-RFLP and FINS methodologies for the identification of commercial fish species in Egypt. Fisheries Research, 185, 34-42.

21. Harshitha, R., & Arunraj, D. R. (2021). Real-time quantitative PCR: A tool for absolute and relative quantification. Biochemistry and Molecular Biology Education, 49(5), 800-812.

22. Nyaruaba, R., Mwaliko, C., Dobnik, D., Neužil, P., Amoth, P., Mwau, M., ... & Wei, H. (2022). Digital PCR applications in the SARS-CoV-2/COVID-19 era: a roadmap for future outbreaks. Clinical Microbiology Reviews, 35(3), e00168-21.

23. Xu, J., Kirtek, T., Xu, Y., Zheng, H., Yao, H., Ostman, E., ... & SoRelle, J. A. (2021). Digital droplet PCR for SARS-CoV-2 resolves borderline cases. American journal of clinical pathology, 155(6), 815-822.

24. Nazir, S. (2023). Medical diagnostic value of digital PCR (dPCR): A systematic review. Biomedical Engineering Advances, 6, 100092.

25. Liu, X., Feng, J., Zhang, Q., Guo, D., Zhang, L., Suo, T., ... & Lan, K. (2020). Analytical comparisons of SARS-COV-2 detection by qRT-PCR and ddPCR with multiple primer/probe sets. Emerging microbes & infections, 9(1), 1175-1179.

26. Vynck, M., Trypsteen, W., Thas, O., Vandekerckhove, L., & De Spiegelaere, W. (2016). The future of digital polymerase chain reaction in virology. Molecular diagnosis & therapy, 20(5), 437-447.

27. Sanders, R., Mason, D. J., Foy, C. A., & Huggett, J. F. (2013). Evaluation of digital PCR for absolute RNA quantification. PloS one, 8(9), e75296.

28. Jones, G. M., Busby, E., Garson, J. A., Grant, P. R., Nastouli, E., Devonshire, A. S., & Whale, A. S. (2016). Digital PCR dynamic range is approaching that of real-time quantitative PCR. Biomolecular detection and quantification, 10, 31-33.

29. Shen, F., Sun, B., Kreutz, J. E., Davydova, E. K., Du, W., Reddy, P. L., ... & Ismagilov, R. F. (2011). Multiplexed quantification of nucleic acids with large dynamic range using multivolume digital RT-PCR on a rotational SlipChip tested with HIV and hepatitis C viral load. Journal of the American Chemical Society, 133(44), 17705-17712.

30. Zhang, L., Gu, C., Ma, H., Zhu, L., Wen, J., Xu, H., ... & Li, L. (2019). Portable glucose meter: trends in techniques and its potential application in analysis. Analytical and bioanalytical chemistry, 411, 21-36.

31. Perry, D. J., Fitzmaurice, D. A., Kitchen, S., Mackie, I. J., & Mallett, S. (2010). Point-of-care testing in haemostasis. British Journal of Haematology, 150(5), 501-514.

32. Shrivastava, S., Trung, T. Q., & Lee, N. E. (2020). Recent progress, challenges, and prospects of fully integrated mobile and wearable point-of-care testing systems for self-testing. Chemical Society Reviews, 49(6), 1812-1866.

33. St-Louis, P. (2000). Status of point-of-care testing: promise, realities, and possibilities. Clinical biochemistry, 33(6), 427-440.

34. Yonel, Z., Kuningas, K., Sharma, P., Dutton, M., Jalal, Z., Cockwell, P., ... & Chapple, I. L. C. (2022). Concordance of three point of care testing devices with clinical chemistry laboratory standard assays and patient-reported outcomes of blood sampling methods. BMC Medical Informatics and Decision Making, 22(1), 248.

35. Heller, D. A., Jin, H., Martinez, B. M., Patel, D., Miller, B. M., Yeung, T. K., ... & Strano, M. S. (2009). Multimodal optical sensing and analyte specificity using single-walled carbon nanotubes. Nature nanotechnology, 4(2), 114-120.

36. Montagnana, M., Caputo, M., Giavarina, D., & Lippi, G. (2009). Overview on self-monitoring of blood glucose. Clinica Chimica Acta, 402(1-2), 7-13.

37. Ghosal, S., Kumar, A., Udutalapally, V., & Das, D. (2021). glucam: Smartphone based blood glucose monitoring and diabetic sensing. IEEE Sensors Journal, 21(21), 24869-24878.

38. Waghmare, A., Parizi, F. S., Hoffman, J., Wang, Y., Thompson, M., & Patel, S. (2023). Glucoscreen: A smartphone-based readerless glucose test strip for prediabetes screening. Proceedings of the ACM on Interactive, Mobile, Wearable and Ubiquitous Technologies, 7(1), 1-20.

39. Doupis, J., Festas, G., Tsilivigos, C., Efthymiou, V., & Kokkinos, A. (2020). Smartphone-based technology in diabetes management. Diabetes Therapy, 11(3), 607-619.

40. Xiang, Y., & Lu, Y. (2011). Using personal glucose meters and functional DNA sensors to quantify a variety of analytical targets. Nature chemistry, 3(9), 697-703.

41. Zhu, X., Sarwar, M., Zhu, J. J., Zhang, C., Kaushik, A., & Li, C. Z. (2019). Using a glucose meter to quantitatively detect disease biomarkers through a universal nanozyme integrated lateral fluidic sensing platform. Biosensors and Bioelectronics, 126, 690-696.

42. Lisi, F., Peterson, J. R., & Gooding, J. J. (2020). The application of personal glucose meters as universal point-of-care diagnostic tools. Biosensors and Bioelectronics, 148, 111835.

43. Li, Z., Uno, N., Ding, X., Avery, L., Banach, D., & Liu, C. (2023). Bioinspired CRISPR-mediated cascade reaction biosensor for molecular detection of HIV using a glucose meter. ACS nano, 17(4), 3966-3975.

44. Park, J., Han, H., Jeung, J. H., Jang, H., Park, C., & Ahn, J. K. (2022). CRISPR/Cas13a-assisted AMP generation for SARS-CoV-2 RNA detection using a personal glucose meter. Biosensors and Bioelectronics: X, 12, 100283.

45. Liu, R., Hu, Y., He, Y., Lan, T., & Zhang, J. (2021). Translating daily COVID-19 screening into a simple glucose test: a proof of concept study. Chemical Science, 12(26), 9022-9030.

46. Abardía-Serrano, C., Miranda-Castro, R., de-Los-Santos-Álvarez, N., & Lobo-Castañón, M. J. (2020). New uses for the personal glucose meter: detection of nucleic acid biomarkers for prostate cancer screening. Sensors, 20(19), 5514.

47. Wu, D., & Lei, X. (2022). Enzymatic cascade reactions for the efficient synthesis of natural products. Tetrahedron, 127, 133099.

48. Ricca, E., Brucher, B., & Schrittwieser, J. H. (2011). Multi-enzymatic cascade reactions: overview and perspectives. Advanced Synthesis & Catalysis, 353(13), 2239-2262.

49. Gloor, J. W., Balakrishnan, L., & Bambara, R. A. (2010). Flap endonuclease 1 mechanism analysis indicates flap base binding prior to threading. Journal of Biological Chemistry, 285(45), 34922-34931.

50. Chapados, B. R., Hosfield, D. J., Han, S., Qiu, J., Yelent, B., Shen, B., & Tainer, J. A. (2004). Structural basis for FEN-1 substrate specificity and PCNA-mediated activation in DNA replication and repair. Cell, 116(1), 39-50.

51. Finger, L. D., Atack, J. M., Tsutakawa, S., Classen, S., Tainer, J., Grasby, J., & Shen, B. (2012). The wonders of flap endonucleases: structure, function, mechanism and regulation. The eukaryotic replisome: a guide to protein structure and function, 301-326.

52. Balakrishnan, L., Gloor, J. W., & Bambara, R. A. (2010). Reconstitution of eukaryotic lagging strand DNA replication. Methods, 51(3), 347-357.

53. Tsutakawa, S. E., Thompson, M. J., Arvai, A. S., Neil, A. J., Shaw, S. J., Algasaier, S. I., ... & Tainer, J. A. (2017). Phosphate steering by Flap Endonuclease 1 promotes 5′-flap specificity and incision to prevent genome instability. Nature communications, 8(1), 15855.

54. Kao, H. I., Henricksen, L. A., Liu, Y., & Bambara, R. A. (2002). Cleavage specificity of Saccharomyces cerevisiae flap endonuclease 1 suggests a double-flap structure as the cellular substrate. Journal of Biological Chemistry, 277(17), 14379-14389.

55. Ayyagari, R., Gomes, X. V., Gordenin, D. A., & Burgers, P. M. (2003). Okazaki fragment maturation in yeast: I. Distribution of functions between FEN1 and DNA2. Journal of Biological Chemistry, 278(3), 1618-1625.

56. Rossi, M. L., Pike, J. E., Wang, W., Burgers, P. M., Campbell, J. L., & Bambara, R. A. (2008). Pif1 helicase directs eukaryotic Okazaki fragments toward the two-nuclease cleavage pathway for primer removal. Journal of Biological Chemistry, 283(41), 27483-27493.

57. Xiang, Y., & Lu, Y. (2012). Using commercially available personal glucose meters for portable quantification of DNA. Analytical chemistry, 84(4), 1975-1980.

58. Kim, H. Y., Ahn, J. K., Park, K. S., & Park, H. G. (2020). Portable glucose meter-based label-free strategy for target DNA detection. Sensors and Actuators B: Chemical, 310, 127808.

59. Kim, H. Y., Park, K. S., & Park, H. G. (2020). Glucose oxidase-like activity of cerium oxide nanoparticles: Use for personal glucose meter-based label-free target DNA detection. Theranostics, 10(10), 4507.

60. Shan, Y., Zhang, Y., Kang, W., Wang, B., Li, J., Wu, X., ... & Liu, F. (2019). Quantitative and selective DNA detection with portable personal glucose meter using loop-based DNA competitive hybridization strategy. Sensors and Actuators B: Chemical, 282, 197-203.

61. Jia, Y., Sun, F., Na, N., & Ouyang, J. (2019). Detection of p53 DNA using commercially available personal glucose meters based on rolling circle amplification coupled with nicking enzyme signal amplification. Analytica Chimica Acta, 1060, 64-70.

62. Wu, T., Cao, Y., Yang, Y., Zhang, X., Wang, S., Xu, L. P., & Zhang, X. (2019). A three-dimensional DNA walking machine for the ultrasensitive dual-modal detection of miRNA using a fluorometer and personal glucose meter. Nanoscale, 11(23), 11279-11284.

63. Ma, W., Liu, M., Xie, S., Liu, B., Jiang, L., Zhang, X., & Yuan, X. (2022). CRISPR/Cas12a system responsive DNA hydrogel for label-free detection of non-glucose targets with a portable personal glucose meter. Analytica Chimica Acta, 1231, 340439.

64. Gong, S., Li, J., Pan, W., Li, N., & Tang, B. (2021). Duplex-specific nuclease-assisted CRISPR-Cas12a strategy for microRNA detection using a personal glucose meter. Analytical Chemistry, 93(30), 10719-10726.

65. Fang, J., Guo, Y., Yang, Y., Yu, W., Tao, Y., Dai, T., ... & Xie, G. (2018). Portable and sensitive detection of DNA based on personal glucose meters and nanogold-functionalized PAMAM dendrimer. Sensors and Actuators B: Chemical, 272, 118-126.

66. Tanifuji, Y., Tong, G., Hiruta, Y., & Citterio, D. (2024). based analytical device for point-of-care nucleic acid quantification combining CRISPR/Cas12a and a personal glucose meter. Analyst, 149(19), 4932-4939.

Abstract in Korean

자가혈당측정기를 이용한 효소 연쇄 반응 기반 핵산 검출 기술 개발

본 논문은 flap endonuclease 1 (FEN1)의 구조 특이적 절단 활성과 연계된 연쇄 효소 반응을 통합한 새로운 분자 진단 플랫폼을 제시합니다. 이 시스템은 중합효소 연쇄 반응(PCR) 증폭 없이 표적 핵산을 검출하며, FEN1 절단으로 생성된 AMP 가포도당 분해를 유도하여 개인용 혈당 측정기(PGM)를 통해 정량화 할 수 있습니다. 우리는 Chlamydia trachomatis (Ct) 서열을 기반으로 한 표적 DNA 를 사용하여 이 플랫폼을 검증했으며, 일반적인 세균 병원체의 서열과 동일한 서열을 검출하는 데 효과적임을 입증했습니다. 본 시스템을 이용하여 표적 핵산을 성공적으로 검출했으며, 검출 한계는 4.8 pM 이었습니다. 또한 Chlamydia trachomatis 에서 유래한 표적 핵산을 검출할 수 있는 가능성을 보였으며, 다른 성병(STD) 유전자 및 불일치 서열에 비해 뛰어난 선택성을 나타냈습니다. PCR 및 형광 기반 기술의 한계를 극복함으로써, 이 플랫폼은 비용 효율적이고 확장 가능하며 사용자 친화적인 진단 솔루션을 제공하며, 자원이 제한된 환경에서의 적용 가능성이 큽니다.

핵심되는 말: Flap endonuclease 1, 연쇄효소반응, 개인혈당측정기, 분자 진단, 현장진단검사